

DOI: 10.1002/ ((please add manuscript number))

Article type: **(Feature Article, Review)**

Graphene-Based Nanomaterials for Flexible and Wearable Supercapacitors

*Liang Huang, Diana Santiago, Patricia Loyselle and Liming Dai**

Dr. L. Huang, Prof. Dr. L. Dai

Center of Advanced Science and Engineering for Carbon (Case4carbon), Department of Macromolecular Science and Engineering, Case Western Reserve University, 10900 Euclid Avenue, Cleveland, OH 44106 (USA)

E-mail: liming.dai@case.edu

Dr. D. Santiago, Dr. P. Loyselle

NASA Glenn Research Center

Materials and Structure Division, 21000 Brookpark Rd, M.S. 106-1, Cleveland, OH 44135 (USA)

Keywords: (graphene nanomaterials, flexible, wearable, supercapacitors)

Along with the rapid development of wearable and flexible electronics, there is an ever increasing demand for lightweight, flexible, and wearable energy storage devices as power sources. Because of the high power density, fast charging/discharging rate, long cycle life and easy fabrication, flexible supercapacitors have been widely explored for this purpose. Graphene-based nanomaterials are promising as electrode materials for flexible supercapacitors due to their extremely large surface area, excellent mechanical and electrical properties, and high electrochemical stability. The two-dimensional structure and high aspect ratio of graphene sheets make them easy to assemble into freestanding films or fibers with robust mechanical properties. In recent years, tremendous progress has been achieved for developing flexible and wearable graphene-based supercapacitors. In this article, we summarize the material and structure design strategies for developing film-shaped and emerging fiber-shaped flexible supercapacitors based on graphene nanomaterials.

1. Introduction

Wearable and flexible electronic products that can be bent, folded or even stretched have received considerable attention.^[1-3] Because they need flexible power sources, there is an urgent need for the development of lightweight, flexible, and wearable energy storage devices.^[1,4] The flexible energy storage devices can be conformal with the deformation while still retaining their electrochemical functions. One of the key challenges to develop flexible energy storage devices is to design and fabricate electrode materials with robust mechanical flexibility, high energy and power density, and excellent cycling stability.

Supercapacitors (SCs), also known as electrochemical capacitors (ECs), are an important class of energy storage devices because of their high power densities (up to 10 kW kg⁻¹) and long cycle life (>100000 cycles).^[5, 6] According to the energy storage mechanism, SCs can be classified as electrochemical double-layer capacitors (EDLCs) and pseudocapacitors.^[6] EDLCs store energies physically by reversible ion adsorption at the electrode/electrolyte interfaces, thus materials with a high surface area are needed to achieve a high capacitance.^[6] On the other hand, pseudocapacitors store energies chemically by fast surface redox reactions of the electrodes.^[6] Because redox reactions are involved in the charge-storage processes, the gravimetric specific capacitance of a pseudocapacitor usually exceeds that of an EDLC, though at the cost of its rate performance and cycling life.^[5,6]

Due to their unique properties, including a large theoretical specific surface area (~2630 m² g⁻¹), high conductivity, good chemical and thermal stability, wide potential window, and excellent mechanical flexibility, graphene-based materials have been extensively explored as electrode materials for flexible supercapacitors.^[7-10] The intrinsic electrochemical double layer capacitance of a single-layer graphene sheet was measured to be ~21 μF cm⁻².^[11] Therefore, if its entire surface area could be fully utilized, a supercapacitor based on graphene is capable of achieving a theoretical electrochemical double layer capacitance up to ~550 F g⁻¹.^[5] In view of several recent review articles on various newly-developed flexible all-solid-

state supercapacitors based on graphene nanomaterials,^[12-17] we will give a focused review on the material and structural design strategies for developing film-shaped and emerging fiber-shaped flexible supercapacitors based on graphene nanomaterials.

2. Film-shaped flexible supercapacitors

2.1. Graphene-based films as platforms for fabricating flexible supercapacitors

The two-dimensional structure and high aspect ratio of graphene sheets make them easy to assemble into freestanding films with robust mechanical properties.^[18-20] By vacuum filtration of graphene dispersion through an Anodisc membrane filter, Chen et al. fabricated graphene papers with a Young's modulus of 41.8 GPa, a tensile strength of 293.3 MPa, an elongation at rupture of 0.8%, and an electrical conductivity as high as 118 S cm⁻¹.^[21] Therefore, graphene-based papers are very promising for flexible supercapacitors. However, graphene sheets are tightly stacked in graphene papers and the electrolytes cannot diffuse into the interlayers of graphene sheets to form electrical double layers, leading to a specific capacitance far below the theoretical value of 500 F g⁻¹ for a graphene paper. Therefore, a number of strategies were developed to prevent aggregation of graphene sheets in graphene-based films in order to increase accessible surface area and promote transport of electrolyte ions.

The first strategy is intercalating some "spacers" such as carbon nanotubes^[22], nanodiamond^[23], polymers^[24-26], and metal oxides^[27,28] between graphene sheets. The resulting composite films can still maintain part of graphene film's excellent mechanical properties while having much higher accessible surface area and facilitated pathways for the diffusion of electrolyte ions, leading to ideal electrode materials for flexible supercapacitors. Many methods have been developed to intercalate "spacers" between graphene sheets, such as layer-by-layer (LBL) self-assembling^[22], vacuum filtration^[23,25] and solution casting^[24]. By LBL electrostatic self-assembling poly(ethyleneimine)-modified graphene sheets with acid-

oxidized CNTs, Yu and Dai fabricated for the first time CNT/rGO hybrid films with CNTs intercalated between rGO sheets.^[22] The resultant hybrid films exhibited a nearly rectangular cyclic voltammogram even at a high scan rate of 1 V s^{-1} and showed an average specific capacitance of 120 F g^{-1} .^[22] By vacuum filtrating a homogeneous dispersion of nanodiamond (ND) and GO, Sun et al prepared a composite GO/ND film with ND intercalated between GO layers.^[23] After graphitizing the composite films at high temperature ($1200 \text{ }^\circ\text{C}$), ND was changed into onion-like carbon (OC) and GO was reduced to conductive rGO. In the resultant graphitic composite films, OC nanoparticles were sandwiched between rGO sheets, which not only prevented the aggregation of rGO sheets but also formed some mesopores (**Figure 1a and b**).^[23] The graphitic composite films thus formed are highly conductive with conductivities as high as 203 S cm^{-1} .^[23] These films are mechanically stable and highly flexible, so they can be directly used as the electrodes for supercapacitors without the addition of a polymer binder or a conductive additive. The supercapacitors showed a specific capacitance as high as 143 F g^{-1} at a discharge rate of 0.2 A g^{-1} .^[23] The composite films also showed high electrochemical stability during repeated charging/discharging cycles, and retained its original specific capacitance ($\sim 100\%$) even after 5000 charge/discharge cycles.

Huang et al., prepared compact rGO/ poly (vinyl pyrrolidone) (PVP) composite films (**Figure 1c**) by casting the stable aqueous mixtures of both components and they have strong mechanical strengths ($121.5 \pm 10.8 \text{ MPa}$) and good flexibility (**Figure 1d**), as well as high electrical conductivities (247.9 S m^{-1}).^[24] The intercalation of poly (vinyl pyrrolidone) (PVP) molecules between rGO sheets can not only effectively prevent the restacking of rGO sheets but also improve the interfacial wettability between the electrodes and electrolyte. PVP has a good affinity with both water and acetonitrile (AN). Thus, both polymer gel electrolytes and organic electrolytes are able to diffuse into the interlayers of graphene sheets to form electrical double layers. The solid-state SCs with a polymer gel electrolyte can exhibit both high gravimetric and volumetric capacitances (168.4 F g^{-1} and 67.4 F cm^{-3} at 1 A g^{-1}) with an

excellent rate capability (76% capacitance retention at 100 A g⁻¹) and a high power density (20 W cm⁻³).^[24] More importantly, these solid-state SCs are highly flexible with only a small fluctuation in capacitance (<10%) after repeatedly bending to 180° around a radius of 2.5 mm for 1,000 cycles.^[24]

Although the theoretical capacitance of graphene can be as high as 550 F g⁻¹ if the entire surface area is used. However, the actual achievable gravimetric specific capacitance is usually lower than 300 F g⁻¹, which leads to a lower energy density.^[7,29,30] Pseudocapacitive materials usually have much higher theoretical capacitances than graphene-based materials, so they will show higher energy density.^[6] The most widely explored pseudocapacitive materials include transition metal oxides^[31,32] and conductive polymers.^[33] Unfortunately, they often suffer from multiple drawbacks, including particle aggregations, poor electrical conductivities (especially for metal oxides), inherent rigidity and structural degradation, leading to a low power density, poor cycling stability, and insufficient flexibility.^[6,12,15] So, the aforementioned pseudocapacitive materials are not suitable for electrodes in flexible supercapacitors. Since graphene possesses a large surface area, high electrical conductivity, light-weight, and flexibility, it can be considered as a suitable framework to support these pseudocapacitive materials. It can be expected that the intercalation of these pseudocapacitive materials between rGO sheets will not only prevent the restacking of rGO sheets but also contribute a great deal of capacitance, thus achieving higher energy density.

Wu et al developed composite films of rGO and polyaniline nanofibers (PANI-NFs) by vacuum filtration the mixed dispersions of both components.^[25] The composite film has a layered structure, and PANI-NFs are sandwiched between rGO layers (**Figure 1e** and **f**). Furthermore, the composite films are mechanically strong and have a high flexibility and good conductivity.^[25] The intercalated PANI-NFs can not only prevent the restacking of rGO sheets but also contribute some pseudocapacitance. Consequently, supercapacitor based on this conductive flexible composite film exhibited a large gravimetric capacitance of 210 F g⁻¹

(discharge rate: 0.3 A g^{-1}). However, the introduction of pseudocapacitance of PANI-NFs results in the decrease of cycling stability and rate capability compared with pure EDLCs.^[25]

2.2. Graphene materials supported by flexible substrates

Another strategy to prevent the restacking of graphene is assembling graphene sheets into three-dimensional (3D) architectures with interconnected porous microstructures, such as graphene hydrogels and aerogels.^[29,30] This unique hierarchical architecture greatly reduced the restacking of graphene sheets and improved the electrochemical performances of graphene-based SCs. However, 3D porous graphene nanomaterials usually have an inflexible structure and show weak mechanical strength, which need to be supported by other substrates for flexible supercapacitors.

El-Kady et al., reported a laser scribed strategy to fabricate 3D porous graphene electrodes by using a commercially available LightScribe CD/DVD optical drive (**Figure 2a**).^[34] During the preparation process, the GO film was reduced to laser scribed graphene (LSG) and simultaneously exfoliated into 3D nanostructures. The resultant 3D porous graphene electrodes showed an open network structure (Figure 2a) and a large accessible specific surface area ($1520 \text{ m}^2 \text{ g}^{-1}$), which is ideal for the diffusion of electrolyte ions.^[34] All-solid-state flexible supercapacitors were assembled by supporting the LSG electrodes with flexible polyethylene terephthalate (PET) substrates and combined them with a PVA– H_3PO_4 polymer gel electrolyte (**Figure 2b**). The CV curves of this device were tested under different bending conditions (**Figure 2c**) and the capacitive behavior did not change even when bent at 180° . Moreover, the stability of the device was tested for more than 1000 cycles while in the bent state, with only $\sim 5\%$ change in the device capacitance. Compared with a single SC, which can only achieve a voltage window of 1.0 V, the tandem series SCs exhibited a 4.0 V charge/discharge voltage window (**Figure 2d**).

The electrical conductivity of LSG electrodes can be sufficiently high (1738 S m^{-1}) to achieve excellent electrochemical performance even without current collectors (using a

nonconductive substrate as mechanical support). However, for most 3D porous graphene electrodes, their electrical conductivities are relatively low, so flexible current collectors are often needed to make flexible supercapacitors. In this context, Xu *et al* ^[35] pressed the functionalized graphene hydrogels (FGHs) onto Au-coated polyimide films, which act as current collectors and flexible substrates at the same time. Although the FGHs were flattened upon pressing, the 3D continuous porous network was still maintained (**Figure 3 b** and **c**) attractive for the polymer gel electrolyte infiltration and ions diffusion.^[35] Then FGH electrodes supported by Au-coated polyimide films were assembled into solid-state flexible supercapacitors by using H₂SO₄-PVA polymer gel electrolyte (**Figure 3d** and **e**). The solid-state SCs exhibited excellent capacitive performances (412 F g⁻¹ at 1 A g⁻¹, 74% capacitance retention at 20 A g⁻¹ and 87% capacitance retention over 10 000 cycles), which are close to the ones using aqueous electrolytes. The FGH-based solid-state supercapacitors also exhibit extraordinary mechanical flexibility in bending tests. The CV curves of the device measured at various bending angles showed almost the same electrochemical behavior even at a large bending angle of 150°. The device durability was further characterized by galvanostatic charge/discharge tests up to 10000 cycles at a high current density of 10 A g⁻¹ under 150° bending angle. Only 13% decay in specific capacitance was observed, highlighting the excellent mechanical and electrical robustness of the interconnected 3D network of FGHs and its favorable interfacial compatibility with polymer gel electrolyte.^[35]

Apart from the capacitance (C), the energy density ($E = 1/2 CV^2$) can also be improved by maximizing the potential window (V) of supercapacitors. A promising way to increase the potential window is to develop asymmetric supercapacitors, which can make full use of the different potential windows of the positive and negative electrodes to increase the operating voltage for a whole device.^[36, 37] In this regard, Choi *et al.* fabricated a solid-state flexible asymmetric supercapacitor with an ionic liquid functionalized chemically modified graphene (IL-CMG) film as the negative electrode and a hydrous RuO₂-IL-CMG composite film as the

positive electrode (**Figure 4**).^[38] The resultant asymmetric supercapacitor operated at a cell voltage up to 1.8 V (**Figure 4c**) and delivered an energy density of 19.7 W h kg⁻¹ and power density of 6.8 kW kg⁻¹. Furthermore, the device showed excellent flexibility and cycling stability, with 95% capacitance retention after 2000 cycles under either bent or twisted condition (**Figure 4d**).

3. Fiber-shaped supercapacitors

As discussed above, various film-shaped solid-state supercapacitors have been developed to meet the practical requirements for flexible SCs, but they usually do not allow for sweat and air from the human body to pass through freely, thus they have limited wearability for potential applications in wearable electronics.^[39] In this regard, a new family of flexible SCs, namely fiber-shaped SCs with 1D fibers as electrodes, has emerged. Because of their unique wire-shaped structure, they are highly flexible and can be woven or knitted into fabrics/textiles with excellent wearability.^[39-44] Such unique architectures also render a great design versatility as compared to conventional film-shaped SCs, since they can be fabricated into various desired shapes and located at different places.^[43,45]

Similar to 2D graphene-based films, 1D graphene-based fibers can also be engineered to be good electrode materials for flexible fiber shaped supercapacitors.^[13,41,42,46-50] Indeed, Li et al. fabricated fiber-shaped graphene electrodes by electrochemically reducing GO on an Au wire.^[42] The rGO sheets were deposited on the surface of the Au wire and assembled into 3D interpenetrating networks (**Figure 5a** and **b**) with a thickness of about 30 μm (**Figure 5c**). The pore sizes of the network are in the range of several micrometers to larger than ten micrometers, and most of the rGO sheets are nearly vertical to the surface of the Au wire (**Figure 5b** and **c**). The micropores in the electrode are fully exposed to the electrolyte for the access of ions to form electrochemical double-layers. The fiber-shaped electrodes were assembled into a solid-state fiber supercapacitor by using the configuration in **Figure 5d**. The

capacitance per unit length of the fiber-shaped flexible supercapacitor was calculated to be $11.4 \mu\text{F cm}^{-1}$. The shape of the CV curves showed a negligible distortion and the capacitance decreased by less than 1% as the SC was bent from 0° to 120° or into the S-shaped structure (**Figure 5e**). Furthermore, the capacitance retention of the SCs after repeated bending to 30° , 60° or 90° for 1000 cycles was measured to be about 96%, 92% or 90%.

The use of Au wire as a fiber-shaped current collector will not only increase the cost and weight of SCs but also restrict the intrinsic flexibility of the device. To address this issue, Meng et al., fabricated a unique all graphene core-sheath fiber, in which a core of graphene fiber (GF) is covered with a sheath of electrochemically deposited 3D porous graphene network (**Figure 6a and b**).^[46] This hierarchically-structured all-graphene hybrid inherits the intrinsic high conductivity and mechanical flexibility of GF in combination with highly exposed surfaces of graphene sheets, thus offering the great advantages as flexible, lightweight electrodes for efficient fiber-shaped supercapacitors. Flexible all-solid-state fiber supercapacitors were built by intertwining two GF@3D-G electrodes with H_2SO_4 -PVA gel electrolyte (**Figure 6c**). The assembled fiber supercapacitor is highly flexible and can be knotted (**Figure 6d**). Interestingly, the fiber supercapacitor can be built to a spring with highly compressible and stretchable properties (**Figure 6e and f**). The fiber supercapacitor can also be conveniently woven into a textile for wearable electronics.^[46]

Scaling up the fabrication process of graphene fibers is a big challenge. Yu et al., developed a scalable method to continuously produce hierarchically structured fibers made of nitrogen-doped rGO hybrids with SWCNTs (**Figure 7a and b**).^[51] The nanocomposite fibers have mesoporous structures of the large specific surface area of $396 \text{ m}^2 \text{ g}^{-1}$ and high conductivity of 102 S cm^{-1} . The resultant fiber type supercapacitor showed a high volumetric capacitance of 300 F cm^{-3} in PVA- H_3PO_4 gel electrolyte (**Figure 7c**). The all-solid-state fiber supercapacitors showed a typical electrical double layer capacitive behavior (**Figure 7d**).

They exhibited high volumetric energy ($\sim 6.3 \text{ mWh cm}^{-3}$, a value comparable to that of 4 V–500 mAh thin-film lithium batteries) while maintaining a power density more than two orders of magnitude higher than that of batteries (**Figure 7e**). The fiber supercapacitors were further subjected to mechanical bending tests. They showed negligible capacitance change ($<0.05\%$) on bending to 90° [51]. Furthermore, it retained more than 97% of its initial capacitance after bending 1,000 times at 90° (**Figure 7f**), demonstrating the high flexibility and electrochemical stability desirable for flexible electronics.^[51]

Liu et al fabricated Ni-coated cotton yarns by electroless deposition of Ni on commercial cotton yarns.^[52] The Ni-coated cotton yarns possessed a high conductivity while keeping the textile-like flexibility, making them as excellent current collectors for flexible fiber supercapacitors. Subsequently, rGO sheets were deposited on the surface of Ni cotton yarns by electrochemically electrolyzing GO aqueous suspension, in which the Ni cotton yarns were used as working electrodes.^[52] In this way, rGO sheets penetrated into the multiple interval spaces among the individual fibers of the Ni-coated cotton yarns. A wearable solid-state SC yarn was assembled with a polyvinyl alcohol (PVA)/LiCl gel, which acted as both the electrolyte and an effective separator of the device (**Figure 8a**). The CV curves of the SC yarn at scanning rates ranging from 5 to 100 mV s^{-1} showed rectangular-like shapes (**Figure 8b**). The shape at high scan rates was similar to those at low scan rates without obvious distortion, indicating a high rate performance and efficient ionic and electronic transports within the electrode materials. In particular, the capacitance of the SC yarn scaled up proportionally as its length increased. As shown in **Figure 8c**, varying the length of the SC yarn from 3 to 17 cm resulted in a linear increase in the device capacitance from 0.28 to 1.52 F. Accordingly, the derived linear capacitance of the SC yarn is 0.11 F cm^{-1} , which is almost 20-fold higher than that of rGO/CNT fiber SC (5.3 mF cm^{-1}).^[52] Remarkably, the volumetric energy density and power density of the all-solid-state SC yarn are 6.1 mWh cm^{-3} and $1,400 \text{ mW cm}^{-3}$,

respectively. As the SC yarn is assembled on the basis of textile materials and solid-state electrolyte, it is ideal for different wearable applications. The composite electrodes could be directly used as threads in commercial embroidery machines (**Figure 8d**). The solid-state SC yarns were woven into a fabric with other pristine cotton yarns in a conventional weaving process (**Figure 8e**).

4. Concluding remarks

Supercapacitors represent one of the major emerging energy storage devices due to their long cycling stability and high power densities. Flexible supercapacitors are receiving tremendous research interest due to the increasing need for flexible and wearable energy storage devices. Graphene-based materials have been extensively investigated as electrode materials for flexible supercapacitors due to their large surface area, excellent mechanical, optical, electrical and electrochemical properties. We have provided a focused review on the material and structure design strategies for fabricating film-shaped and fiber-shaped flexible supercapacitors based on graphene nanomaterials.

Although impressive progress has been achieved for graphene-based flexible and wearable supercapacitors, there remain some challenges for practical applications of these electrode materials. Freestanding compact graphene-based paper electrodes exhibit high electrical conductivity and excellent mechanical flexibility, but they have only moderate rate stability and power density due to limited porous structures. In contrast, 3D porous graphene-based electrodes show excellent rate and power performance, while they usually have limited mechanical strength and need some flexible support substrate to endow them with flexibility. Fiber shaped supercapacitors are highly flexible and can be woven or knitted into fabrics/textiles with excellent wearability. However, the large-scale production of graphene-based fibers with high conductivity and quality at low cost is still challenging. Although flexible supercapacitor based on graphene nanomaterials were reported to show excellent

performance in small-scale devices, it is still a big question that if this good performance can still be maintained in industry-scale big devices.

Acknowledgements

The authors are grateful for the financial support from NASA (NNC16CA42C), NSF (CMMI-1400274).

Received: ((will be filled in by the editorial staff))

Revised: ((will be filled in by the editorial staff))

Published online: ((will be filled in by the editorial staff))

References

- [1] W. Liu, M. S. Song, B. Kong, Y. Cui, *Adv. Mater.* **2017**, *29*, 1603436.
- [2] T.-H. Han, H. Kim, S.-J. Kwon, T.-W. Lee, *Mater. Sci. Eng. R Rep.* **2017**, *118*, 1-43.
- [3] J. S. Heo, J. Eom, Y.-H. Kim, S. K. Park, *Small*, **2018**, *14*, 1703034.
- [4] X. Wang, X. Lu, B. Liu, D. Chen, Y. Tong, G. Shen, *Adv. Mater.* **2014**, *26*, 4763-4782.
- [5] J. Chen, C. Li, G. Shi, *J. Phys. Chem. Lett.* **2013**, *4*, 1244-1253.
- [6] P. Simon, Y. Gogotsi, *Nat. Mater.* **2008**, *7*, 845-854.
- [7] M. D. Stoller, S. Park, Y. Zhu, J. An, R. S. Ruoff, *Nano Lett.* **2008**, *8*, 3498-3502.
- [8] T. Chen, Y. H. Xue, A. K. Roy, L. Dai, *ACS Nano* **2014**, *8*, 1039-1046.
- [9] J. K. Sun, Y. H. Li, Q. Y. Peng, S. C. Hou, D. C. Zou, Y. Y. Shang, Y. B. Li, P. X. Li, Q. J. Du, Z. H. Wang, Y. Z. Xia, L. H. Xia, X. L. Li, A. Y. Cao, *ACS Nano* **2013**, *7*, 10225-10232.
- [10] Y. Yang, Q. Y. Huang, L. Y. Niu, D. R. Wang, C. Yan, Y. Y. She, Z. J. Zheng, *Adv. Mater.* **2017**, *29*, 1606679.
- [11] J. L. Xia, F. Chen, J. H. Li, N. J. Tao, *Nat. Nanotechnol.* **2009**, *4*, 505-509.
- [12] Y. L. Shao, M. F. El-Kady, L. J. Wang, Q. H. Zhang, Y. G. Li, H. Z. Wang, M. F. Mousavi, R. B. Kaner, *Chem. Soc. Rev.* **2015**, *44*, 3639-3665.

- [13] Q. Yang, Z. Xu, C. Gao, *J. Energy Chem.* **2018**, *27*, 6-11.
- [14] L. Chen, Y. Liu, Y. Zhao, N. Chen, L. Qu, *Nanotechnology* **2016**, *27*, 032001.
- [15] T. Chen, L. Dai, *J. Mater. Chem. A* **2014**, *2*, 10756-10775.
- [16] W. K. Chee, H. N. Lim, Z. Zainal, N. M. Huang, I. Harrison, Y. Andou, *J. Phys. Chem. C* **2016**, *120*, 4153-4172.
- [17] L. L. Liu, Z. Q. Niu, J. Chen, *Chem. Soc. Rev.* **2016**, *45*, 4340-4363.
- [18] D. A. Dikin, S. Stankovich, E. J. Zimney, R. D. Piner, G. H. Dommett, G. Evmenenko, S. T. Nguyen, R. S. Ruoff, *Nature* **2007**, *448*, 457-460.
- [19] D. Li, M. B. Müller, S. Gilje, R. B. Kaner, G. G. Wallace, *Nat. Nanotechnol.* **2008**, *3*, 101-105.
- [20] G. Wang, X. Sun, F. Lu, H. Sun, M. Yu, W. Jiang, C. Liu, J. Lian, *Small*, **2012**, *8*, 452-459..
- [21] H. Chen, M. B. Müller, K. J. Gilmore, G. G. Wallace, D. Li, *Adv. Mater.* **2008**, *20*, 3557-3561.
- [22] D. Yu, L. Dai, *J. Phys. Chem. Lett.* **2010**, *1*, 467-470.
- [23] Y. Sun, Q. Wu, Y. Xu, H. Bai, C. Li, G. Shi, *J. Mater. Chem.* **2011**, *21*, 7154-7160.
- [24] L. Huang, C. Li, G. Q. Shi, *J. Mater. Chem. A* **2014**, *2*, 968-974.
- [25] Q. Wu, Y. X. Xu, Z. Y. Yao, A. R. Liu, G. Q. Shi, *ACS Nano* **2010**, *4*, 1963-1970.
- [26] N. A. Kumar, H. J. Choi, Y. R. Shin, D. W. Chang, L. M. Dai, J. B. Baek, *ACS Nano* **2012**, *6*, 1715-1723.
- [27] L. Peng, Y. Zhu, H. Li, G. Yu, *Small*, **2016**, *12*, 6183-6199.
- [28] A. Chidembo, S. H. Aboutalebi, K. Konstantinov, M. Salari, B. Winton, S. A. Yamini, I. P. Nevirkovets, H. K. Liu, *Energy Environ. Sci.* **2012**, *5*, 5236-5240.
- [29] Y. X. Xu, Z. Y. Lin, X. Q. Huang, Y. Liu, Y. Huang, X. F. Duan, *ACS Nano* **2013**, *7*, 4042-4049.

- [30] Z. Weng, Y. Su, D.-W. Wang, F. Li, J. Du, H.-M. Cheng, *Adv. Energy Mater.* **2011**, *1*, 917-922.
- [31] N. L. Wu, *Mater. Chem. Phys.* **2002**, *75*, 6-11.
- [32] T. Brousse, M. Toupin, R. Dugas, L. Athouel, O. Crosnier, D. Belanger, *J. Electrochem. Soc.* **2006**, *153*, 2171-2180.
- [33] A. Rudge, J. Davey, I. Raistrick, S. Gottesfeld, J. P. Ferraris, *J. Power Sources* **1994**, *47*, 89-107.
- [34] M. F. El-Kady, V. Strong, S. Dubin, R. B. Kaner, *Science* **2012**, *335*, 1326-30.
- [35] Y. Xu, Z. Lin, X. Huang, Y. Wang, Y. Huang, X. Duan, *Adv. Mater.* **2013**, *25*, 5779-5784.
- [36] N. Choudhary, C. Li, J. Moore, N. Nagaiah, L. Zhai, Y. Jung, J. Thomas, *Adv. Mater.* **2017**, *29*, 1605336.
- [37] C. Yang, J. Shen, C. Wang, H. Fei, H. Bao, G. Wang, *J. Mater. Chem. A* **2014**, *2*, 1458-1464.
- [38] B. G. Choi, S. J. Chang, H. W. Kang, C. P. Park, H. J. Kim, W. H. Hong, S. Lee, Y. S. Huh, *Nanoscale* **2012**, *4*, 4983-4988.
- [39] D. Yu, Q. Qian, L. Wei, W. Jiang, K. Goh, J. Wei, J. Zhang, Y. Chen, *Chem. Soc. Rev.* **2015**, *44*, 647-662.
- [40] Y. Hu, H. Cheng, F. Zhao, N. Chen, L. Jiang, Z. Feng, L. Qu, *Nanoscale* **2014**, *6*, 6448-6451.
- [41] L. Lim, Y. Liu, W. Liu, R. Tjandra, L. Rasenthiram, Z. Chen, A. Yu, *ACS Appl. Mater. Interfaces* **2017**, *9*, 39576-39583.
- [42] Y. Li, K. Sheng, W. Yuan, G. Shi, *Chem. Commun.* **2013**, *49*, 291-293.
- [43] G. X. Qu, J. L. Cheng, X. D. Li, D. M. Yuan, P. N. Chen, X. L. Chen, B. Wang, H. S. Peng, *Adv. Mater.* **2016**, *28*, 3646-3652.

- [44] H. H. Cheng, Z. L. Dong, C. G. Hu, Y. Zhao, Y. Hu, L. T. Qu, N. Chena, L. M. Dai, *Nanoscale* **2013**, *5*, 3428-3434.
- [45] T. Chen, R. Hao, H. Peng, L. Dai, *Angew. Chem. Int. Ed.* **2015**, *54*, 618-622.
- [46] Y. Meng, Y. Zhao, C. Hu, H. Cheng, Y. Hu, Z. Zhang, G. Shi, L. Qu, *Adv. Mater.* **2013**, *25*, 2326-2331.
- [47] J. L. Yu, M. Wang, P. Xu, S. H. Cho, J. Suhr, K. Gong, L. H. Meng, Y. D. Huang, J. H. Byun, Y. Oh, Y. S. Yan, T. W. Chou, *Carbon* **2017**, *119*, 332-338.
- [48] Y. Liang, Z. Wang, J. Huang, H. H. Cheng, F. Zhao, Y. Hu, L. Jiang, L. T. Qu, *J. Mater. Chem. A* **2015**, *3*, 2547-2551.
- [49] X. Li, T. Zhao, Q. Chen, P. Li, K. Wang, M. Zhong, J. Wei, D. Wu, B. Wei, H. Zhu, *Phys. Chem. Chem. Phys.* **2013**, *15*, 17752-17757.
- [50] Q. Chen, Y. Meng, C. Hu, Y. Zhao, H. Shao, N. Chen, L. Qu, *J. Power Sources* **2014**, *247*, 32-39.
- [51] D. S. Yu, K. Goh, H. Wang, L. Wei, W. C. Jiang, Q. Zhang, L. M. Dai, Y. Chen, *Nat. Nanotechnol.* **2014**, *9*, 555-562.
- [52] L. B. Liu, Y. Yu, C. Yan, K. Li, Z. J. Zheng, *Nat. Commun.* **2015**, *6*, 7260.

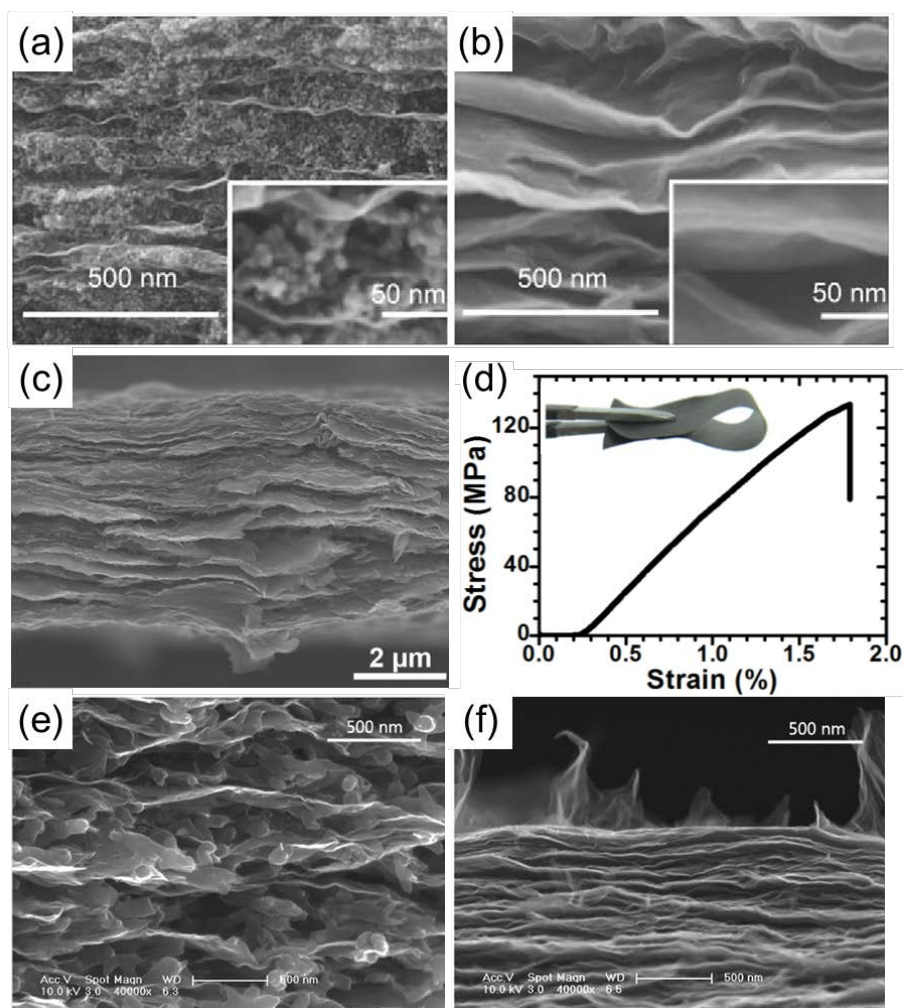


Figure 1. Cross-section SEM images of onion-like carbon/ CCG composite film (a) and pure CCG film (b). Reproduced with permission.^[23] Copyright 2011, Royal Society of Chemistry. (c) Cross-section SEM images of rGO/PVP composite film, (d) The typical stress-strain curve of an rGO/PVP composite film. Inset is the photograph of a flexible rGO/PVP composite film. Reproduced with permission.^[24] Copyright 2014, Royal Society of Chemistry. Cross-section SEM images of PANI nanofibers/CCG composite film (e) and CCG film (f). Reproduced with permission.^[25] Copyright 2010, American Chemistry Society.

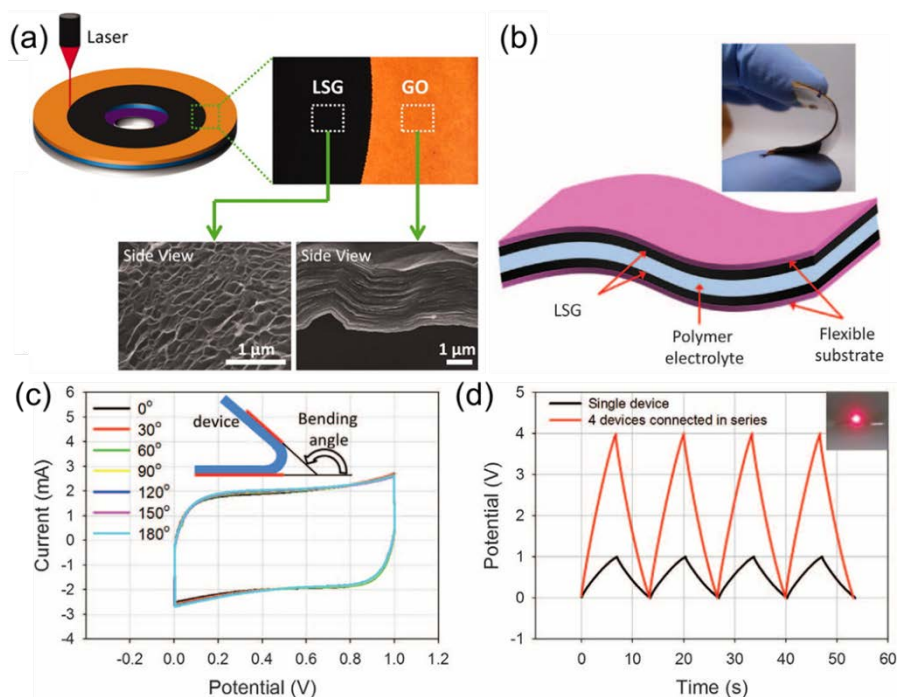


Figure 2. (a) The low-power infrared laser reduces brown GO film to black laser-scribed graphene (LSG) film. The cross-sectional SEM images show that stacked GO sheets change into well-exfoliated few-layered LSG film. (b) A schematic diagram of the all-solid-state LSG-EC illustrates that the gelled electrolyte can serve as both the electrolyte and separator. (Inset) A digital photograph showing the flexibility of the device. (c) Bending the device has almost no effect on its performance, as seen in these CVs collected at a scan rate of 1000 mV s^{-1} . (d) Galvanostatic charge/discharge curves for four tandem ECs connected in series. Reproduced with permission.^[34] Copyright 2012, The American Association for the Advancement of Science.

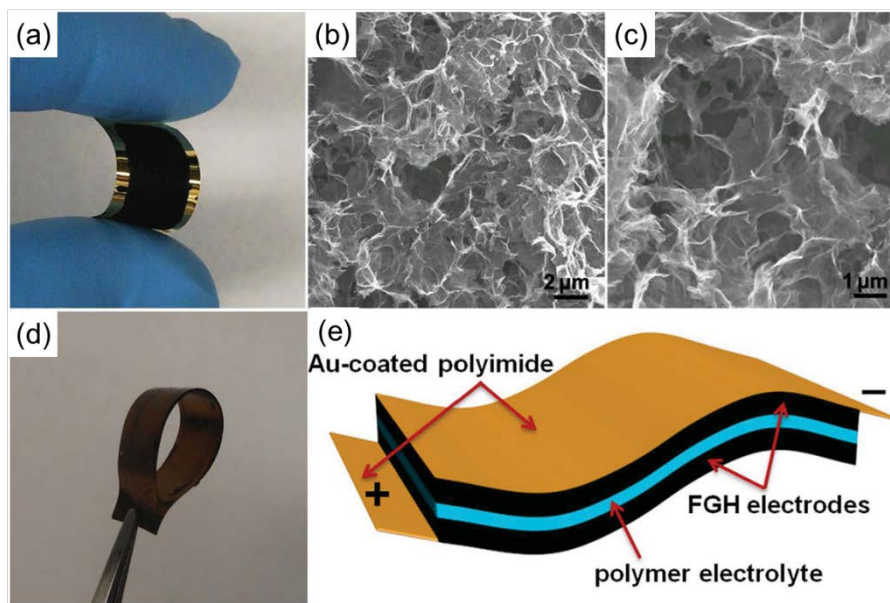


Figure 3. (a) Digital photograph of a flexible functionalized graphene hydrogels (FGHs) thin film electrode. (b) Low- and (c) high magnification SEM images of interior microstructures of the FGH film. (d) Digital photograph of an FGH-based flexible solid-state supercapacitor. (e) A schematic diagram of the solid-state device with H_2SO_4 -PVA polymer gel as the electrolyte and separator. Reproduced with permission.^[35] Copyright 2013, Wiley-VCH.

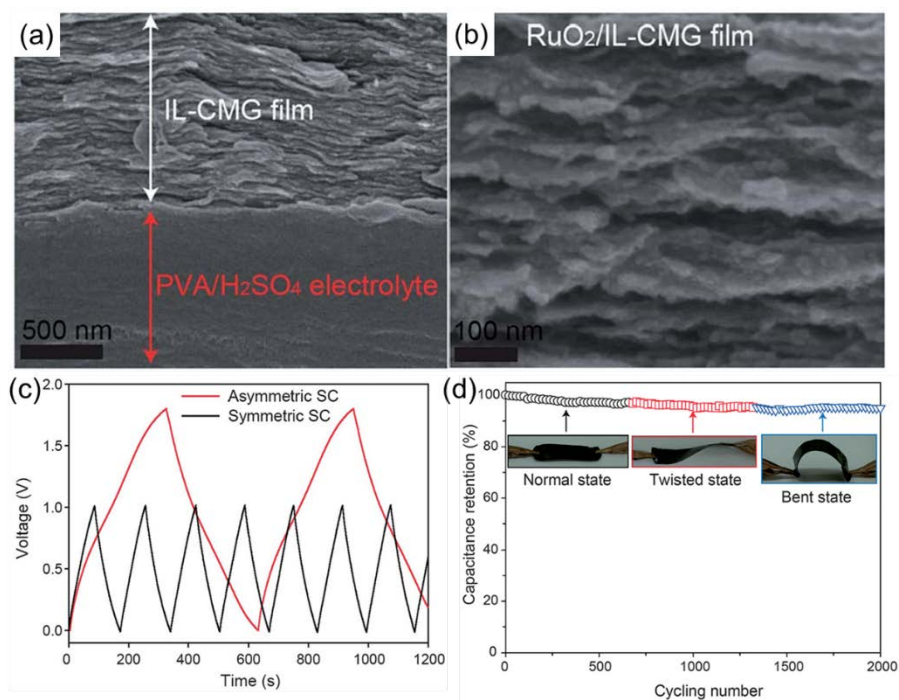


Figure 4. Cross-sectional SEM images of (a) the interface between the IL-CMG film and PVA–H₂SO₄ electrolyte and (b) RuO₂–ILCMG film in an asymmetrical supercapacitors device. (c) Galvanostatic charge-discharge curves with a constant current density of 1 A/g for asymmetrical SC and symmetric IL-CMG-based SC devices. (d) Long-term cycling stability of asymmetrical SC devices under normal, twisted, and bent states with a constant current density of 1 A/g over 2000 cycles. Reproduced with permission.^[38] Copyright 2012, Royal Society of Chemistry.

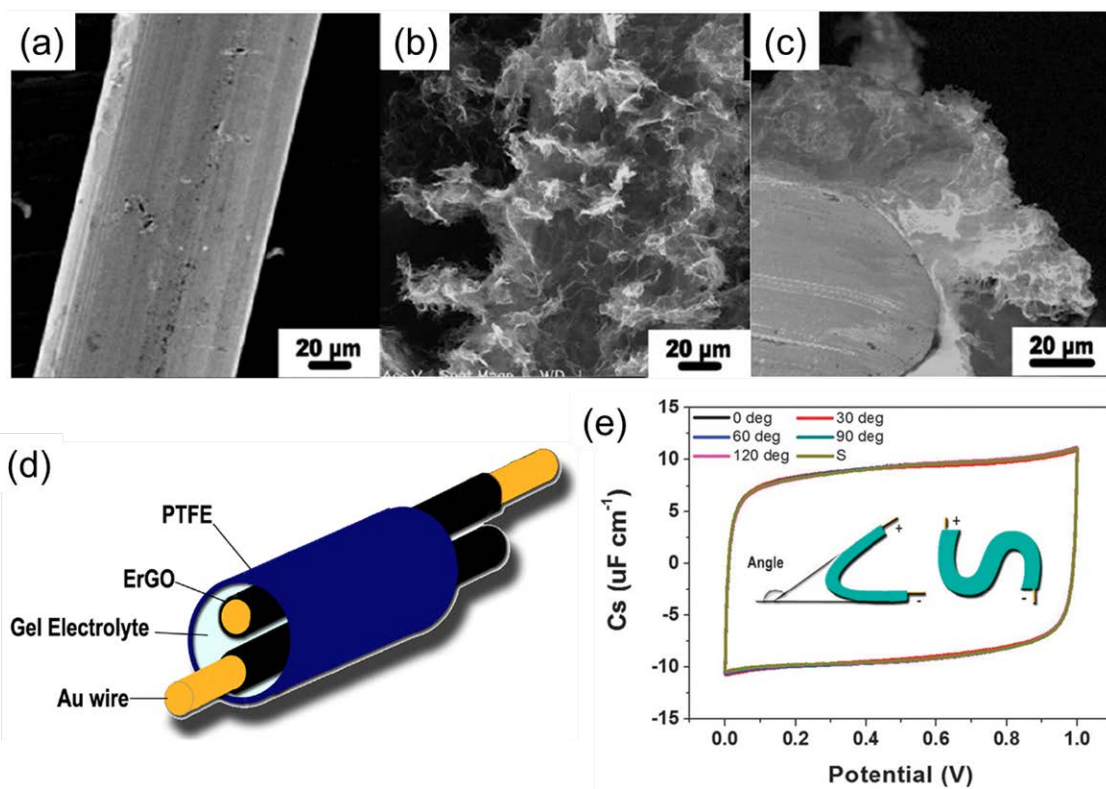


Figure 5. SEM images of (a) an Au wire and (b) an ErGO/Au electrode. (c) Cross-section SEM images of an ErGO/Au electrode. (d) The schematic diagram of a fiber-shaped solid SC. (e) CV curves of the typical fiber-shaped solid SC at different bending angles. Reproduced with permission.^[42] Copyright 2013, Royal Society of Chemistry.

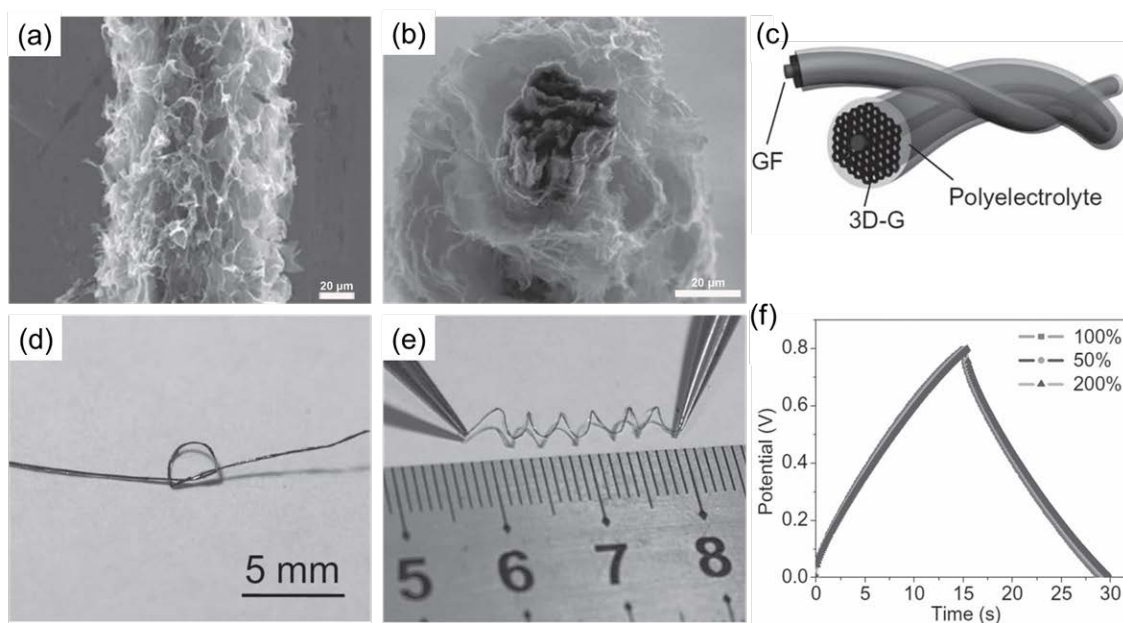


Figure 6. (a) SEM images of a GF@3D-G. (b) Cross-section view of a GF@3D-G showing the core GF surrounding with standing graphene sheets. (c) Schematic illustration of a wire-shaped supercapacitor fabricated from two twined GF@3D-Gs with the polyelectrolyte. (d) A photo of the knotted fiber supercapacitor of GF@3D-Gs. (e) The spring-like supercapacitor with an effective GF@3D-G length of ca. 4.5 cm at stretched (ca. 200%) status. (f) The corresponding charge/discharge curves of the spring-like supercapacitor at free (100%), compressed (ca. 50%) and stretched (ca. 200%) status, respectively. The applied current is 4 μA . Reproduced with permission.^[46] Copyright 2013, Wiley-VCH.

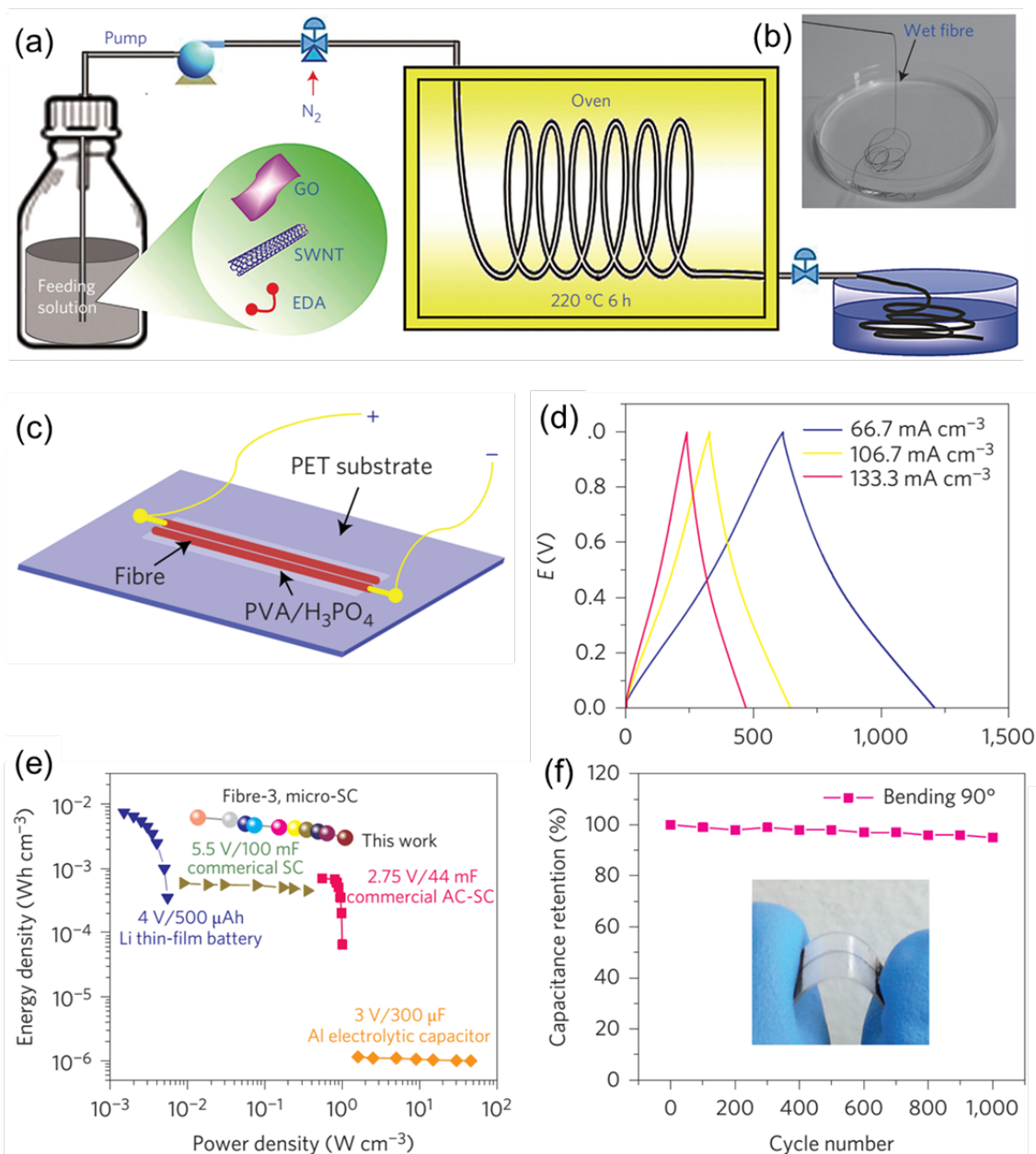


Figure 7. (a) Schematic of the synthesis of carbon hybrid microfibers. (b) Photograph of the as-prepared fibers collected in water. (c) Schematic of a micro-SC constructed using two fiber electrodes on a polyester (PET) substrate. (d) Galvanostatic charge/discharge curves at various current densities. (e) Energy and power densities of the micro-SC compared with commercially available state-of-the-art energy storage systems. (f) Capacitance retention after 1,000 cycles up to a 90° bending angle. Inset is the photograph of a bent micro-SC. Reproduced with permission.^[51] Copyright 2014, Macmillan Publishers Limited.

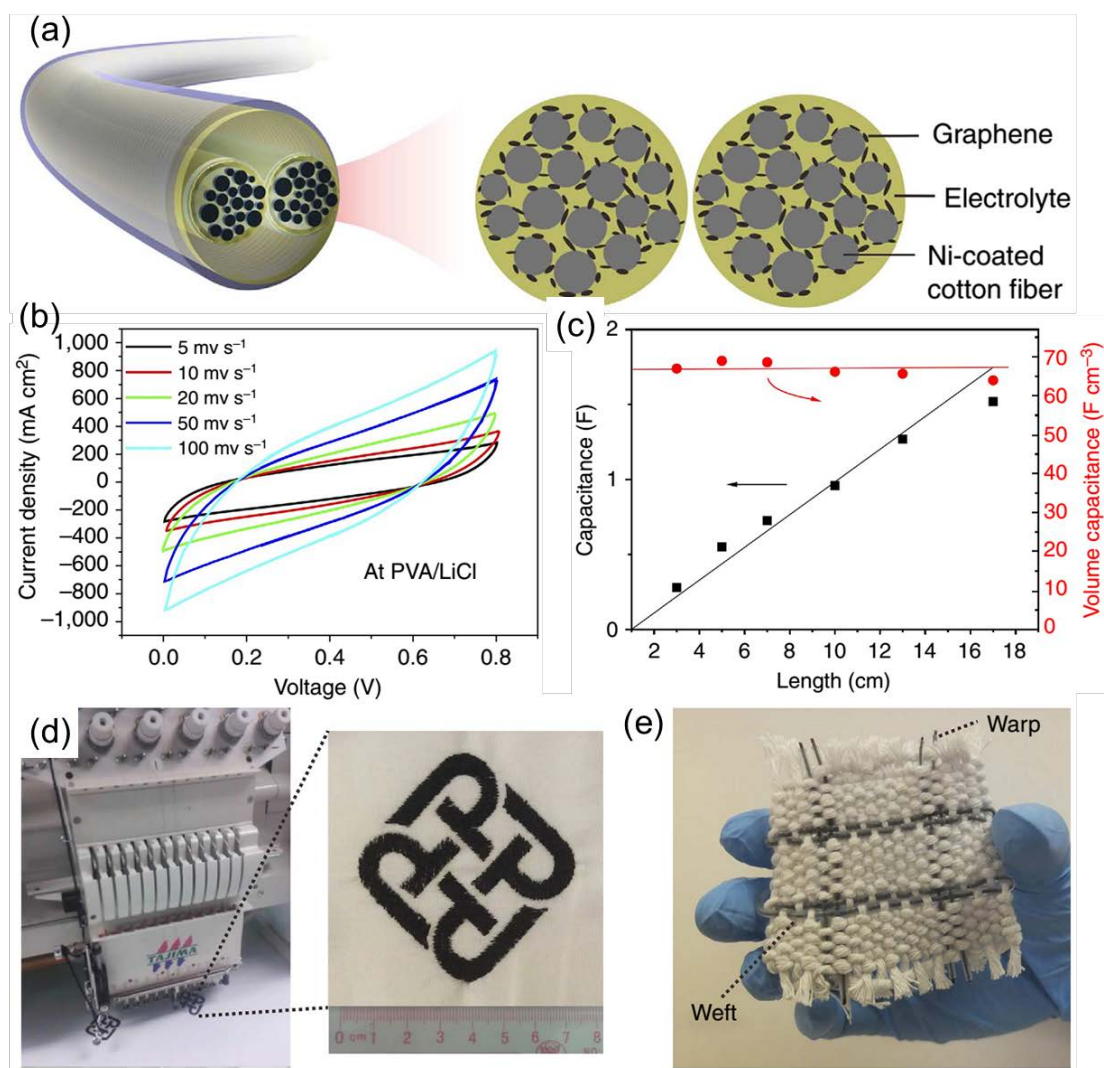
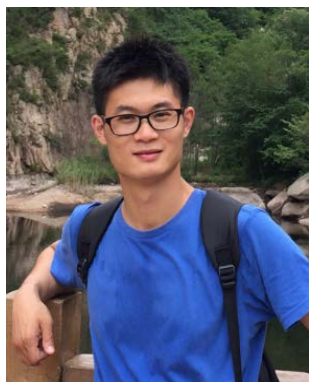


Figure 8. (a) Schematic illustration of the structure of one SC yarn. (b) CV curves of the device at various scan rates. (c) Device capacitance as a function of the device length. (d) Digital images of embroidery logos using the composite electrode yarns. (e) A woven fabric made with solid-state SC yarns. Reproduced with permission.^[52] Copyright 2015, Macmillan Publishers Limited.

Author biographies



Liming Dai is the Kent Hale Smith Professor at Case Western Reserve University and is also director of the Center of Advanced Science and Engineering for Carbon (Case4Carbon). He received a BSc from Zhejiang University in 1983, a PhD from Australian National University in 1991, and did his postdoctoral research at the Cavendish Laboratory in Cambridge. His research activities cover the synthesis and device fabrication of conjugated polymers and carbon nanomaterials for energy and bio-related applications.



Liang Huang obtained his BS from Beijing University of Chemical Technology in 2011, and his Ph.D from Tsinghua University in 2016. He is currently a postdoctoral research associate in Professor Liming Dai's group at Case Western Reserve University. His current research interests are the fabrication of graphene-based membranes and their applications.



Diana Santiago is a Research Materials Engineer of the Materials Chemistry and Physics Branch from NASA Glenn Research Center for seven years. She received her BS in Chemistry from University of Puerto Rico at Cayey in 2003, and her PhD from University of Puerto Rico at Rio Piedras in 2012. She is currently the co-principal investigator of the Multifunctional Structures for High Energy Lightweight Load-bearing Storage (M-SHELLS), and has been working on the preparation and modification of nanomaterials for different applications.



Patricia Loyselle has worked in various aspects of fuel cell and battery technology for 28 years at the NASA Glenn Research Center. She received Ph.D from Michigan Technological University in 1990. During her career, she has been involved in the research and development of advanced battery materials, battery designs and test and integration. She has also been involved in fuel cell activities ranging from basic research and development of materials and components to power system design, test and integration for space and terrestrial systems.

The table of contents entry should be 50–60 words long, and the first phrase should be bold.

Graphene-based nanomaterials usually exhibit extremely large specific surface area, excellent mechanical and electrical properties as well as high electrochemical stability, which make them promising as electrode materials for flexible and wearable supercapacitors. Here the material and structure design strategies for developing film-shaped and emerging fiber-shaped flexible supercapacitors based on graphene nanomaterials are summarized.

Keyword

graphene nanomaterials, flexible, wearable, supercapacitors

L. Huang and L. Dai*

Title

Graphene-Based Nanomaterials for Flexible and Wearable Supercapacitors

ToC figure ((Please choose one size: 55 mm broad \times 50 mm high **or** 110 mm broad \times 20 mm high. Please do not use any other dimensions))

